

Gravastars with an Interior Dark Energy Fluid Forming a Naked Singularity

C. F. C. Brandt ^{2,*} R. Chan ^{1,†} M.F.A. da Silva ^{2,‡} and P. Rocha ^{2,§}

¹ *Coordenação de Astronomia e Astrofísica,*

Observatório Nacional, Rua General José Cristino, 77,

São Cristóvão 20921-400, Rio de Janeiro, RJ, Brazil

² *Departamento de Física Teórica, Instituto de Física,*

Universidade do Estado do Rio de Janeiro, Rua São Francisco Xavier 524,

Maracanã 20550-900, Rio de Janeiro, RJ, Brasil

³ *IST - Instituto Superior de Tecnologia de Paracambi,*

FAETEC, Rua Sebastião de Lacerda s/n,

Bairro da Fábrica, Paracambi, 26600-000, RJ, Brazil

(Dated: November 3, 2018)

Abstract

We consider a gravastar model made of anisotropic dark energy with an infinitely thin spherical shell of a perfect fluid with the equation of state $p = (1 - \gamma)\sigma$ with an external de Sitter-Schwarzschild region. It is found that in some cases the models represent the "bounded excursion" stable gravastars, where the thin shell is oscillating between two finite radii, while in other cases they collapse until the formation of black holes or naked singularities. An interesting result is that we can have black hole and stable gravastar formation even with an interior and a shell constituted of dark and repulsive dark energy, as also shown in previous work. Besides, in one case we have a dynamical evolution to a black hole (for $\Lambda = 0$) or to a naked singularity (for $\Lambda > 0$). This is the first time in the literature that a naked singularity emerges from a gravastar model.

PACS numbers: 98.80.-k,04.20.Cv,04.70.Dy

*Electronic address: fredcharret@yahoo.com.br

†Electronic address: chan@on.br

‡Electronic address: mfasnic@gmail.com

§Electronic address: pedroennarocha@gmail.com

I. INTRODUCTION

Nowadays, although we know that gravastars are not an alternative to black holes, these theoretical objects cannot be ignored and, in fact, they have received a considerable attention [1][8]-[12].

The pioneer model of gravastar was proposed by Mazur and Mottola (MM) [4], consisting of five layers: an internal core $0 < R < R_1$, described by the de Sitter universe, an intermediate thin layer of stiff fluid $R_1 < R < R_2$, an external region $R > R_2$, described by the Schwarzschild solution, and two infinitely thin shells, appearing, respectively, on the hypersurfaces $R = R_1$ and $R = R_2$, where R denotes the radius of the star. The intermediate layer is constructed in such way that R_1 is inner than the de Sitter horizon, while R_2 is outer than the Schwarzschild horizon, eliminating the apparent horizon. Configurations with a de Sitter interior have long history which we can find, for example, in the work of Dymnikova and Galaktionov [5]. After this work, Visser and Wiltshire [6] pointed out that there are two different types of stable gravastars which are stable gravastars and “bounded excursion” gravastars. In the spherically symmetric case, the motion of the surface of the gravastar can be written in the form [6],

$$\frac{1}{2}\dot{R}^2 + V(R) = 0, \quad (1)$$

where $\dot{R} \equiv dR/d\tau$, with τ being the proper time of the surface. Depending on the properties of the potential $V(R)$, we can have two kinds of gravastars, which are (i) Stable gravastars and (ii) “Bounded excursion” gravastars. For the former one there must exist a radius R_0 such that $V(R_0) = 0$, $V'(R_0) = 0$, $V''(R_0) > 0$, where a prime denotes the ordinary differentiation with respect to the indicated argument. If and only if there exists such a radius R_0 for which the above conditions are satisfied, the model is said to be stable.

On the other hand, for the second one, there exist two radii R_1 and R_2 such that $V(R_1) = 0$, $V'(R_1) \leq 0$, $V(R_2) = 0$, $V'(R_2) \geq 0$, with $V(R) < 0$ for $a \in (R_1, R_2)$, where $R_2 > R_1$.

Many authors have studied the stability of the gravastar models for several equations of state, among them we can mention [6] - [9]. Some generalizations of these models can be found in the literature [10] - [19].

The study of gravastar, in general, has considered these objects embedded in a Schwarzschild spacetime (except in the references [7] and [11]). However, taking the cosmological point of view that the universe must be fullfilled by a considerable amount of dark

energy, it is very important to investigate its influence in the gravastar stability and in its possible dynamic evolution. In a first step, we have considered the de Sitter-Schwarzschild exterior spacetime, in order to introduce a positive cosmological constant, which has been suggested as a dark energy candidate.

In this paper, we generalize our previous works [11]-[13] to the case where the equation of state of the infinitely thin shell is still given by $p = (1 - \gamma)\sigma$ with γ being a constant, the interior consists of an anisotropic dark energy fluid (similarly used in [13]), while the exterior is now the de Sitter-Schwarzschild space (similarly used in [11]). In the previous work [13] we showed that anisotropic dark energy could collapse forming a black hole or a gravastar. We also studied the effect of anisotropy of the interior fluid on the formation of gravastars and it was concluded that the sign of the difference between the pressures (radial and tangential) affects the conditions of the formation of the gravastar and black holes when the interior fluid of prototype gravastars is anisotropic. This is confirmed in this present work.

Here we shall first construct three-layer dynamical models, and then show both types of gravastars and black holes exist for various situations. In addition, this model shows that a naked singularity can be the final stage of a gravastar. The rest of the paper is organized as follows: In Sec. II we present the metrics of the interior and exterior spacetimes, and write down the motion of the thin shell in the form of equation (1). In Sec. III we show the definitions of dark and phantom energy, for the interior fluid and for the shell. In Sec. IV we discuss the different structures that are formed from standard or dark energy anisotropic fluid. Finally, in Sec. V we present our conclusions.

II. DYNAMICAL THREE-LAYER PROTOTYPE GRAVASTARS

The interior fluid is made of an anisotropic dark energy fluid with a metric given by the first Lobo's model [19]

$$ds_i^2 = -f_1 dt^2 + f_2 dr^2 + r^2 d\Omega^2, \quad (2)$$

where $d\Omega^2 \equiv d\theta^2 + \sin^2(\theta)d\phi^2$, and

$$\begin{aligned} f_1 &= (1 - 2ar^2)^{-\frac{1+3\omega}{2}}, \\ f_2 &= \frac{1}{1 - 2ar^2}, \end{aligned} \quad (3)$$

where ω is a constant, and its physical meaning can be seen from the following equation (5). Since the mass is given by $\bar{m}(r) = 4\pi\rho_0 r^3/3$ and $a = 4\pi\rho_0/3$ then we have that $a > 0$, where ρ_0 is the homogeneous energy density. Note that there is a horizon at $r_h = 1/\sqrt{2a}$, thus the radial coordinate must obey $r < r_h$. The corresponding energy density ρ , radial and tangential pressures p_r and p_t are given, respectively, by

$$\begin{aligned} \rho &= \rho_0 = \text{constant}, \\ p_r &= \omega\rho_0, \\ p_t &= \omega\rho_0 \left[1 + \frac{4\pi(1+\omega)(1+3\omega)\rho_0 r^2}{6\omega(1-\frac{8\pi\rho_0}{3}r^2)} \right], \end{aligned} \quad (4)$$

$$(5)$$

when $\omega = -1$ and $\omega = -1/3$ we obtain an interior isotropic pressure fluid.

The exterior spacetime is given by the de Sitter-Schwarzschild metric

$$ds_e^2 = -fdv^2 + f^{-1}d\mathbf{r}^2 + \mathbf{r}^2 d\Omega^2, \quad (6)$$

where $f = 1 - \frac{2m}{r} - (\mathbf{r}/L_e)^2$ and $L_e = \sqrt{3/\Lambda_e}$. The metric of the hypersurface on the shell is given by

$$ds_\Sigma^2 = -d\tau^2 + R^2(\tau)d\Omega^2, \quad (7)$$

where τ is the proper time.

Since $ds_i^2 = ds_e^2 = ds_\Sigma^2$, we find that $r_\Sigma = \mathbf{r}_\Sigma = R$, and

$$f_1 \dot{t}^2 - f_2 \dot{r}_\Sigma^2 = 1, \quad (8)$$

$$f \dot{v}^2 - \frac{\dot{\mathbf{r}}_\Sigma^2}{f} = 1, \quad (9)$$

where the dot denotes the ordinary differentiation with respect to the proper time. On the other hand, the interior and exterior normal vectors to the thin shell are given by

$$\begin{aligned} n_\alpha^i &= (-\dot{r}_\Sigma, \dot{t}, 0, 0), \\ n_\alpha^e &= (-\dot{\mathbf{r}}_\Sigma, \dot{v}, 0, 0). \end{aligned} \quad (10)$$

Then, the interior and exterior extrinsic curvatures, using the junction condition $r_\Sigma = \mathbf{r}_\Sigma = R$ and equations (8), (9) calculated at the shell radius, are given by

$$\begin{aligned} K_{\tau\tau}^i &= -(1 - 2aR^2)^{-(3\omega+1)/2} \left\{ \left[6(1 - 2aR^2)^{(3\omega+1)/2} \dot{R}^2 \omega + 6aR^2 \dot{t}^2 \omega + 2aR^2 \dot{t}^2 - 3\dot{t}^2 \omega - \dot{t}^2 \right] \right. \\ &\quad \left. \times aR\dot{t} - (1 - 2aR^2)^{(3\omega+1)/2} (-1 + 2aR^2) (\dot{R}\ddot{t} - \ddot{R}\dot{t}) \right\} (-1 + 2aR^2)^{-1}, \end{aligned} \quad (11)$$

$$K_{\theta\theta}^i = \dot{t}(1 - 2aR^2)R, \quad (12)$$

$$K_{\phi\phi}^i = K_{\theta\theta}^i \sin^2(\theta), \quad (13)$$

$$K_{\tau\tau}^e = \dot{v}[(2L_e^2 m \dot{v} + L_e^2 R \dot{R} - L_e^2 R \dot{v} + R^3 \dot{v})(2L_e^2 m \dot{v} - L_e^2 R \dot{R} - L_e^2 R \dot{v} + R^3 \dot{v}) - 2L_e^4 R^2 \dot{R}^2][(2m - R)L_e^2 + R^3]^{-1}(L_e^2 m - R^3)L_e^{-4}R^{-3} + \dot{R}\ddot{v} - \ddot{R}\dot{v} \quad (14)$$

$$K_{\theta\theta}^e = -\dot{v}((2m - R)L_e^2 + R^3)L_e^{-2} \quad (15)$$

$$K_{\phi\phi}^e = K_{\theta\theta}^e \sin^2(\theta). \quad (16)$$

Since [20]

$$[K_{\theta\theta}] = K_{\theta\theta}^e - K_{\theta\theta}^i = -M, \quad (17)$$

where M is the mass of the shell, we find that

$$M = \dot{v}R \left[1 - \frac{2m}{R} - \left(\frac{R}{L_e} \right)^2 \right] + \dot{t}(1 - 2aR^2)R. \quad (18)$$

Then, substituting equations (8) and (9) into (18) we get

$$M = -R \left[1 - \frac{2m}{R} - \left(\frac{R}{L_e} \right)^2 + \dot{R}^2 \right]^{1/2} + R \frac{(1 - 2aR^2 + \dot{R}^2)^{1/2}}{(1 - 2aR^2)^{-(3\omega+2)/2}}. \quad (19)$$

In order to keep the ideas of MM as much as possible, we consider the thin shell as consisting of a fluid with the equation of state, $p = (1 - \gamma)\sigma$, where σ and p denote, respectively, the surface energy density and pressure of the shell and γ is a constant. Then, the equation of motion of the shell is given by [20]

$$\dot{M} + 8\pi R \dot{R} p = 4\pi R^2 [T_{\alpha\beta} u^\alpha n^\beta] = 4\pi R^2 (T_{\alpha\beta}^e u_e^\alpha n_e^\beta - T_{\alpha\beta}^i u_i^\alpha n_i^\beta), \quad (20)$$

where u^α is the four-velocity.

Let us first calculate $T_{\alpha\beta}^e u_e^\alpha n_e^\beta - T_{\alpha\beta}^i u_i^\alpha n_i^\beta$. We can get the energy-momentum tensor from reference [19] given by

$$T_{\alpha\beta}^i = (\rho + p_t)u_\alpha^i u_\beta^i + p_t g_{\alpha\beta} + (p_r - p_t)\chi_\alpha \chi_\beta, \quad (21)$$

where u_α^i is the timelike four-velocity vector ($u_\alpha^i u_i^\alpha = -1$), χ_α is the unit spacelike vector in the radial direction ($\chi_\alpha \chi^\alpha = 1$), n_α^i is the spacelike normal vector $n_\alpha^i n_i^\alpha = \frac{1}{f_1 f_2}$ ($f_1 > 0$ and $f_2 > 0$), in the region filled with the anisotropic fluid. Thus, we have

$$u_\alpha^i \chi^\alpha = 0, \quad (22)$$

and

$$n_{\alpha}^i u_i^{\alpha} = 0. \quad (23)$$

Thus, since $T_{\alpha\beta}^e = 0$, we can easily proof that $T_{\alpha\beta}^e u_e^{\alpha} n_e^{\beta} - T_{\alpha\beta}^i u_i^{\alpha} n_i^{\beta} = 0$. Thus,

$$\dot{M} + 8\pi R \dot{R} (1 - \gamma) \sigma = 0. \quad (24)$$

Recall that $\sigma = M/(4\pi R^2)$, we find that equation (24) has the solution

$$M = k R^{2(\gamma-1)}, \quad (25)$$

where k is an integration constant. Substituting equation (25) into equation (19), and rescaling m , $L_e a$ and R as,

$$\begin{aligned} m &\rightarrow m k^{-\frac{1}{2\gamma-3}}, \\ a &\rightarrow a k^{\frac{2}{2\gamma-3}}, \\ L_e &\rightarrow L_e k^{\frac{2}{2\gamma-3}}, \\ R &\rightarrow R k^{-\frac{1}{2\gamma-3}}, \end{aligned} \quad (26)$$

we find that it can be written in the form of equation (1) with a replaced by R , and

$$\begin{aligned} V(R, m, L_e, \omega, a, \gamma) = & \\ & -\frac{1}{2R^2 L_e^2 (b^2 - 1)} \left[2R^{2\gamma-2} b L_e \left(\frac{1}{b^2 - 1} \right) \left(R^{2\gamma-2} b L_e - \right. \right. \\ & \left. \left. \sqrt{2m L_e^2 R + R^4 - 2R^4 L_e^2 a + L_e^2 R^{4\gamma-4} - 2b^2 m L_e^2 R - b^2 R^4 + 2R^4 L_e^2 a b^2} \right) \right. \\ & \left. + R^2 L_e^2 - R^2 L_e^2 b^2 + 2R^4 L_e^2 a b^2 - 2m L_e^2 R - R^4 - L_e^2 R^{4\gamma-4} \right] \end{aligned} \quad (27)$$

where

$$b \equiv (1 - 2aR^2)^{-(1+3\omega/2)}. \quad (28)$$

Clearly, for any given constants m , ω , a and γ , equation (27) uniquely determines the collapse of the prototype gravastar. Depending on the initial value R_0 , the collapse can form either a black hole, a gravastar, a de Sitter, or a spacetime filled with anisotropic dark energy fluid. In the last case, the thin shell first collapses to a finite non-zero minimal radius and then expands to infinity.

The exterior horizons are given by [23]

$$r_{bh} = \frac{2m}{\sqrt{3y}} \cos\left(\frac{\pi + \psi}{3}\right), \quad (29)$$

$$r_c = \frac{2m}{\sqrt{3y}} \cos\left(\frac{\pi - \psi}{3}\right), \quad (30)$$

where $y = (m/L_e)^2$, $\psi = \arccos(3\sqrt{3y})$, r_{bh} denotes the black hole horizon and r_c denotes the cosmological horizon.

To guarantee that initially the spacetime does not have any kind of horizons, cosmological or event, we must restrict R_0 to the range,

$$r_{bh} < R_0 < r_h \text{ or } r_c, \quad (31)$$

where R_0 is the initial collapse radius. When $m = 0 = a$, the thin shell disappears, and the whole spacetime is Minkowski. So, in the following we shall not consider this case.

Since the potential (27) is so complicated, it is too difficult to study it analytically. Instead, in the following we shall study it numerically.

III. CLASSIFICATIONS OF MATTER, DARK ENERGY, AND PHANTOM ENERGY FOR ANISOTROPIC FLUIDS

Recently [22], the classification of matter, dark and phantom energy for an anisotropic fluid in terms of the energy conditions was studied since the pressure components may play very important roles and can have quite different contributions. In this paper, we will use this classification to study the collapse of the dynamical prototype gravastars, constructed in the last section. The denomination used for each kind of fluid is given in Table 1.

In order to consider the equations (2) and (5) for describing dark energy stars we must analyze carefully the ranges of the parameter ω that in fact furnish the expected fluids. It can be shown that the condition $\rho + p_r > 0$ is violated for $\omega < -1$ and fulfilled for $\omega > -1$, for any values of R and b . The conditions $\rho + p_t > 0$ and $\rho + p_r + 2p_t > 0$ are satisfied for $\omega < -1$ and $-1/3 < \omega < 0$, for any values of R and b . For the other intervals of ω the energy conditions depend on very complicated relations of R and b [22]. This provides an explicit example, in which the definition of dark energy must be dealt with great care. Another case was provided in a previous work [22].

In order to fulfill the energy condition $\sigma + 2p \geq 0$ of the shell and assuming that $p = (1 - \gamma)\sigma$ we must have $\gamma \leq 3/2$. On the other hand, in order to satisfy the condition $\sigma + p \geq 0$, we obtain $\gamma \leq 2$. Hereinafter, we will use only some particular values of the parameter γ which are analyzed in this work. See Table II.

TABLE I: This table summarizes the classification of the interior matter field, based on the energy conditions [21], where we assume that $\rho \geq 0$.

Matter	Condition 1	Condition 2	Condition 3
Standard Matter	$\rho + p_r + 2p_t \geq 0$	$\rho + p_r \geq 0$	$\rho + p_t \geq 0$
Dark Energy	$\rho + p_r + 2p_t < 0$	$\rho + p_r \geq 0$	$\rho + p_t \geq 0$
Repulsive Phantom Energy	$\rho + p_r + 2p_t < 0$	$\rho + p_r < 0$	$\rho + p_t \geq 0$
		$\rho + p_r \geq 0$	$\rho + p_t < 0$
Attractive Phantom Energy	$\rho + p_r + 2p_t \geq 0$	$\rho + p_r < 0$	$\rho + p_t \geq 0$
		$\rho + p_r \geq 0$	$\rho + p_t < 0$
		$\rho + p_r < 0$	$\rho + p_t < 0$

TABLE II: This table summarizes the classification of matter on the thin shell, based on the energy conditions [21]. The last column indicates the particular values of the parameter γ , where we assume that $\rho \geq 0$.

Matter	Condition 1	Condition 2	γ
Standard Matter	$\sigma + 2p \geq 0$	$\sigma + p \geq 0$	-1 or 0
Dark Energy	$\sigma + 2p < 0$	$\sigma + p \geq 0$	7/4
Repulsive Phantom Energy	$\sigma + 2p < 0$	$\sigma + p < 0$	3

In the next sections we will discuss the different possibilities for the type of system that can be formed from the study of the potential $V(R, m, L_e, \omega, a, \gamma)$: black hole of standard matter or dark energy, stable or "bounded excursion" gravastar and even naked singularity.

IV. STRUCTURES FORMED

Here we can find many types of systems, depending on the combination of the constitution matter of the shell and core. Among them, there are formation of black holes, stable and "bounded excursion" gravastars, as it has already shown in our previous works [8]-[12], and even a naked singularity constituted exclusively of dark energy. All of them are listed in the table III.

As can be seen in the figure 1, depending on the value of the cosmological constant, we can see that $V(R) = 0$ now can have one, two or three real roots. Then, we have, say, R_i , where $R_{i+1} > R_i$. For $L_e = L_1$ (corresponding to $\Lambda = 0$) If we choose $R_0 > R_3$ none structure is allowed in this region because the potential is greater than the zero. However, if we choose $R_2 < R_0 < R_3$, the collapse will bounce back and forth between $R = R_1$ and $R = R_2$. Such a possibility is better shown in the figure 9. This is exactly the so-called "bounded excursion" model mentioned in [6], and studied in some details in [8]-[12]. Of course, in a realistic situation, the star will emit both gravitational waves and particles, and the potential will be self-adjusted to produce a minimum at $R = R_{static}$ where $V(R = R_{static}) = 0 = V'(R = R_{static})$ whereby a gravastar is finally formed [6, 8–10]. For $R_0 < R_1$ a black hole is formed in the end of the collapse of the shell.

The scenario above can significantly be changed if we consider $\Lambda > 0$. In this case for $L_e > L_c$, we also have bounded excursion gravastars if $R_2 < R_0 < R_3$. However, for $R_0 < R_1$ the final structure can be now a black hole or a naked singularity since the presence of the cosmological constant above a certain limit (L_e^*) eliminates the event horizon (its radius becomes negative), as can be seen in the table IV. See figures 4, 5 and 6. This is the first evidence of a naked singularity formation from a gravastar model. Moreover for $L_e = L_c$, then $R_2 = R_3$, a stable gravastar is formed if $R_0 = R_2$, while for $L_e < L_c$ there is only one real root. Note that for any value of $L_e > L_e^*$, a naked singularity is formed for small initial radius of the shell.

Another two very interesting structures that arise from this model are a black hole, represented by figures 7, 10, 15 and 16, and a stable gravastar, represented by figure 14, all of them made of dark energy. It is remarkable that the stable gravastar is constituted only by phantom energy. It means that a system constituted only by dark energy is able to achieve an equilibrium state or even to collapse. Thus, solving equation (19) for $\dot{R}(\tau)$ we can integrate $\dot{R}(\tau)$ and obtain $R(\tau)$, which are shown in the figures 3, 8, 11 and 12 for the case F.

V. CONCLUSIONS

In this paper, we have studied the problem of the stability of gravastars by constructing dynamical three-layer models of VW [6], which consists of an internal anisotropic dark energy

TABLE III: This table summarizes all possible kind of energy of the interior fluid and of the shell and compares the formed structures in the two gravastar models ($\Lambda = 0$, $\Lambda > 0$). The letters SG, UG, BEG, BH, NS and N denote stable gravastar, unstable gravastar, bounded excursion gravastar, black hole, naked singularity and none, respectively.

Case	Interior Energy	Shell Energy	Figures	Structures ($\Lambda = 0$)	Structures ($\Lambda > 0$)
A	Standard	Standard		BH	BH
B	Standard	Dark		BH	BH
C	Standard	Repulsive Phantom		UG/BH	BH
D	Dark	Standard		SG	N
E	Dark	Dark	15	UG/BH	BH
F	Dark	Repulsive Phantom	1,2,4,5,6,7,9 10,13	BH/BEG BH/UG	BEG/SG/NS BH
G	Repulsive Phantom	Standard		BH	BH
H	Repulsive Phantom	Dark	16	BH	BH
I	Repulsive Phantom	Repulsive Phantom	14	SG	N
J	Attractive Phantom	Standard		N	N
K	Attractive Phantom	Dark		N	N
L	Attractive Phantom	Repulsive Phantom		N	N

fluid, a dynamical infinitely thin shell of perfect fluid with the equation of state $p = (1 - \gamma)\sigma$, and an external de Sitter-Schwarzschild spacetime.

We have shown explicitly that the final output can be a black hole, a "bounded excursion" stable gravastar depending on the total mass m of the system, the cosmological constant L_e , the parameter ω , the constant a , the parameter γ and the initial position R_0 of the dynamical shell. All these possibilities have non-zero measurements in the phase space of m , L_e , a , ω , γ and R_0 . All the results can be summarized in Table III.

An interesting result that we can deduce from Table III is that we can have black hole and stable gravastar formation even with an interior and a shell constituted of dark and repulsive dark energy (cases E, F, H and I).

We also would like to point out the significant influence of the presence of the exterior cosmological constant to formation of this kind of structure. Note that in the case I, rep-

TABLE IV: Radii r_{bh} and r_c calculated using equation (29) as a function of L_e for $L_e < L_c$ and for $L_e > L_c$ where $m = 10^{-9}$ and $L_c = 61.49177124$.

r_{bh}	r_c	L_e
$0.2072568092 \times 10^{-8}$	1.0	1.0
$0.4589337770 \times 10^{-8}$	5.0	5.0
$0.9178675538 \times 10^{-8}$	10.0	10.0
		L_e^*
$-0.4736659684 \times 10^{-8}$	20.0	20.0
$-0.7104989528 \times 10^{-8}$	30.0	30.0
$-0.9473319370 \times 10^{-7}$	40.0	40.0
$-0.1184164921 \times 10^{-7}$	50.0	50.0
$-0.1456327969 \times 10^{-7}$	61.49177126	L_c
$-0.1657830889 \times 10^{-7}$	70.0	70.0
$-0.1894663874 \times 10^{-7}$	80.0	80.0
$-0.2131496858 \times 10^{-7}$	90.0	90.0
$-0.2368329842 \times 10^{-7}$	1.0×10^2	1.0×10^2
$-0.2368329842 \times 10^{-6}$	1.0×10^3	1.0×10^3
$-0.2368329842 \times 10^{-5}$	1.0×10^4	1.0×10^4
$-0.2368329842 \times 10^{-4}$	1.0×10^5	1.0×10^5
$-0.2368329842 \times 10^{-3}$	1.0×10^6	1.0×10^6
$-0.2368329842 \times 10^{-2}$	1.0×10^7	1.0×10^7
$-0.2368329842 \times 10^{-1}$	1.0×10^8	1.0×10^8
-2.368329842	1.0×10^{10}	1.0×10^{10}
-2.368329842×10^1	1.0×10^{11}	1.0×10^{11}
-2.368329842×10^2	1.0×10^{12}	1.0×10^{12}
$-0.2368329842 \times 10^{13}$	1.0×10^{22}	1.0×10^{22}
$-0.2368329842 \times 10^{81}$	1.0×10^{90}	1.0×10^{90}
$-\infty$	∞	∞

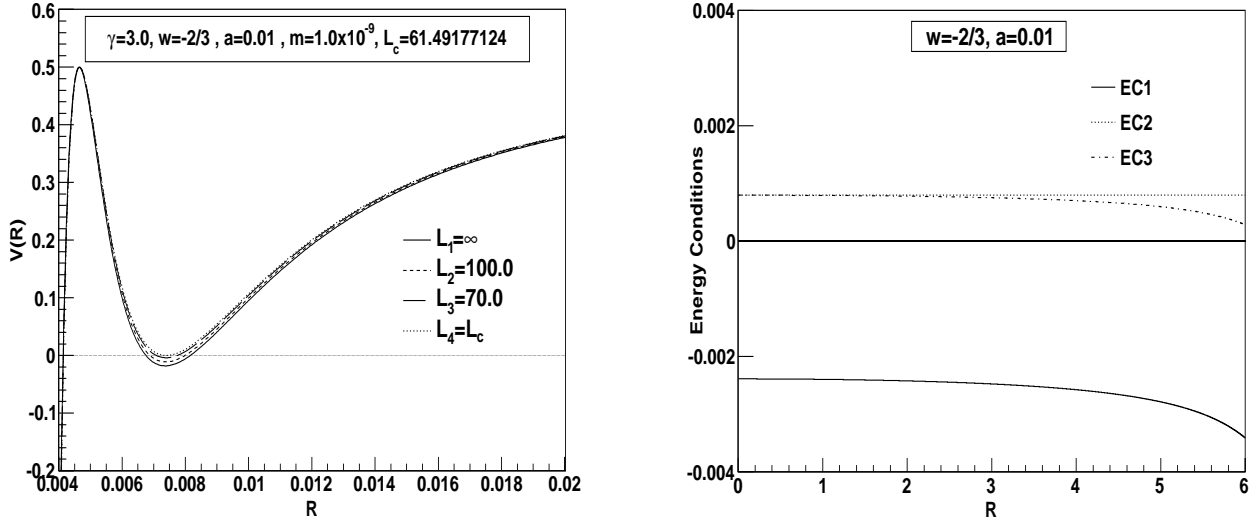


FIG. 1: The potential $V(R)$ and the energy conditions $EC1 \equiv \rho + p_r + 2p_t$, $EC2 \equiv \rho + p_r$ and $EC3 \equiv \rho + p_t$, for $\gamma = 3$, $\omega = -2/3$, $a = 0.01$ and $m_c = 0.1054688609 \times 10^{-8}$. The horizons are: $r_h = 7.071067814$; $r_{bh} = -0.2368329842 \times 10^{-7}$, $r_c = 99.99999998$ ($L_e = 100$); $r_{bh} = -0.1657830889 \times 10^{-7}$, $r_c = 70$ ($L_e = 70$); $r_{bh} = -0.1456327969 \times 10^{-7}$, $r_c = 61.49177126$ ($L_e = 61.49177124$). Note that we have a gravastar enclosing a naked singularity. Then, for small R , the shell can collapse to form a naked singularity. **Case F**

resented by figure 14, we have a stable gravastar (for $\Lambda = 0$) or no formed structure (for $\Lambda > 0$), as well as in the case D, where we have a traditional stable gravastar only for $\Lambda = 0$. Still more interesting is the case F, represented by figure 1, where for small radius of the shell we have formation of a black hole (for $\Lambda = 0$) or a naked singularity (for $\Lambda > 0$). This is the first time in the literature that a naked singularity emerges from a gravastar model. Besides, the figures 3, 8, 11 and 12 give us examples of the dynamical evolution of a gravastar to a naked singularity, a "bounded excursion" gravastar, a black hole and an unstable gravastar, respectively.

Acknowledgments

The financial assistance from FAPERJ/UERJ (MFAdaS) are gratefully acknowledged. The author (RC) acknowledges the financial support from FAPERJ (no. E-26/171.754/2000,

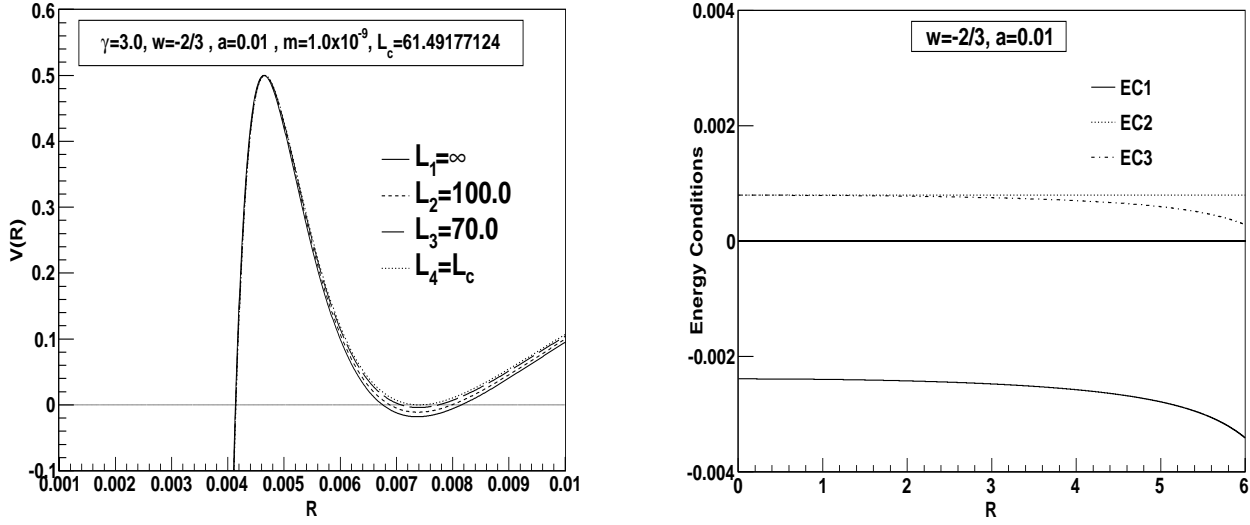


FIG. 2: The zoom of the potential $V(R)$ (figure 1) and the energy conditions $EC1 \equiv \rho + p_r + 2p_t$, $EC2 \equiv \rho + p_r$ and $EC3 \equiv \rho + p_t$, for $\gamma = 3$, $\omega = -2/3$, $a = 0.01$ and $m_c = 0.1054688609 \times 10^{-8}$. The horizons are: $r_h = 7.071067814$; $r_{bh} = -0.2368329842 \times 10^{-7}$, $r_c = 99.99999998$ ($L_e = 100$); $r_{bh} = -0.1657830889 \times 10^{-7}$, $r_c = 70$ ($L_e = 70$); $r_{bh} = -0.1456327969 \times 10^{-7}$, $r_c = 61.49177126$ ($L_e = 61.49177124$). Note that we have a gravastar enclosing a naked singularity. Then, for small R , the shell can collapse to form a naked singularity. **Case F**

E-26/171.533/2002 and E-26/170.951/2006). The authors (RC and MFAdaS) also acknowledge the financial support from Conselho Nacional de Desenvolvimento Científico e Tecnológico - CNPq - Brazil. The author (MFAdaS) also acknowledges the financial support from Financiadora de Estudos e Projetos - FINEP - Brazil (Ref. 2399/03).

[1] D. Horvat and S. Ilijic [arXiv:07071636]; P. Marecki [arXiv:gr-qc/0612178]; F.S.N. Lobo, Phys. Rev. D **75**, 024023 (2007) [arXiv:gr-qc/0612030]; Class. Quantum Grav. **23**, 1525 (2006); F.S.N. Lobo, Aaron V. B. Arellano, *ibid.*, **24**, 1069 (2007); T. Faber [arXiv:gr-qc/0607029]; C. Cattoen [arXiv:gr-qc/0606011]; O.B. Zaslavskii, Phys. Lett. B **634**, 111 (2006); C. Cattoen, T. Faber, and M. Visser, Class. Quantum Grav. **22**, 4189 (2005).

[2] E.J. Copeland, M. Sami and S. Tsujikawa, Int. J. Mod. Phys. D **15**, 1753 (2006); T. Padman-

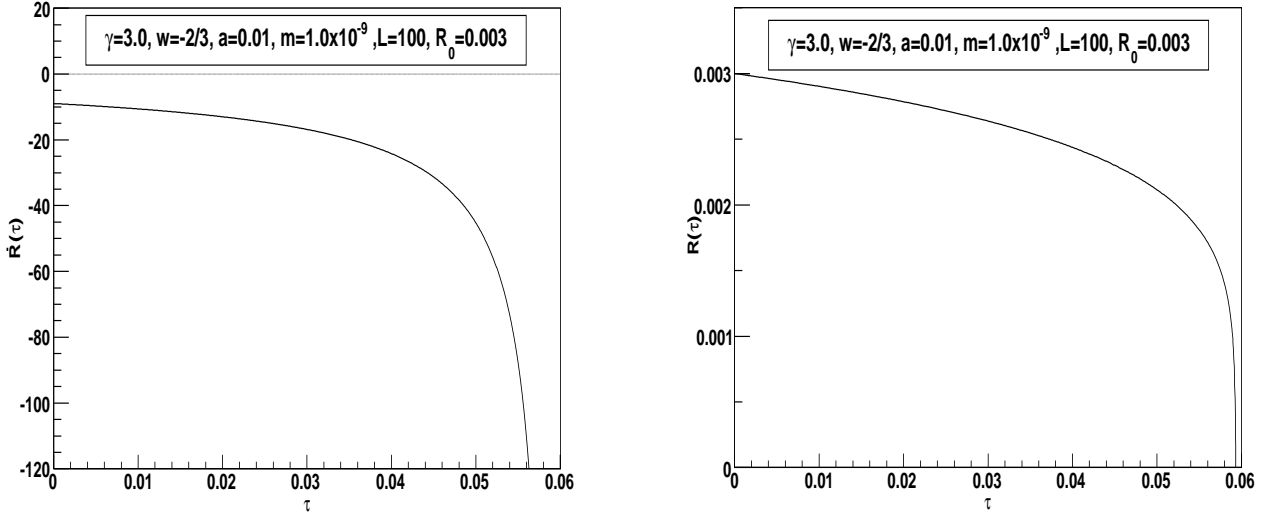


FIG. 3: These figures represent the dynamical evolution of a gravastar to a naked singularity for the potential given by the figure 2, assuming $R_0 = R(0) = 0.003$.

abhan [arXiv:07052533].

- [3] A.E. Broderick and R. Narayan, *Class. Quantum Grav.* **24**, 659 (2007) [arXiv:gr-qc/0701154].
- [4] P.O. Mazur and E. Mottola (2001) arXiv:gr-qc/0109035; *Proc. Nat. Acad. Sci.* **101**, 9545 (2004) [arXiv:gr-qc/0407075].
- [5] I. Dymnikova and E. Galaktionov, *Physics Letters B* **645**,358 (2007) and references herein.
- [6] M. Visser and D.L. Wiltshire, *Class. Quantum Grav.* **21**, 1135 (2004)[arXiv:gr-qc/0310107].
- [7] B.M.N. Carter, *Class. Quantum Grav.* **22**, 4551 (2005) [arXiv:gr-qc/0509087].
- [8] P. Rocha, A.Y. Miguelote, R. Chan, M.F. da Silva, N.O. Santos, and A. Wang, ”*Bounded excursion stable gravastars and black holes*,” *J. Cosmol. Astropart. Phys.* **6**, 25 (2008) [arXiv:gr-qc/08034200].
- [9] P. Rocha, R. Chan, M.F. da Silva and A. Wang, ”*Stable and ”Bounded Excursion” Gravastars, and Black Holes in Einstein’s Theory of Gravity*,” *J. Cosmol. Astropart. Phys.* **11**, 10 (2008) [arXiv:gr-qc/08094879].
- [10] R. Chan, M.F. da Silva, P. Rocha and A. Wang, ”*Stable Gravastars with Anisotropic Dark Energy*”, *J. Cosmol. Astropart. Phys.* **3**, 10 (2009) [arXiv:gr-qc/08124924].
- [11] R. Chan, M.F.A. da Silva and P. Rocha, ”*How the cosmological constant affects gravastar*

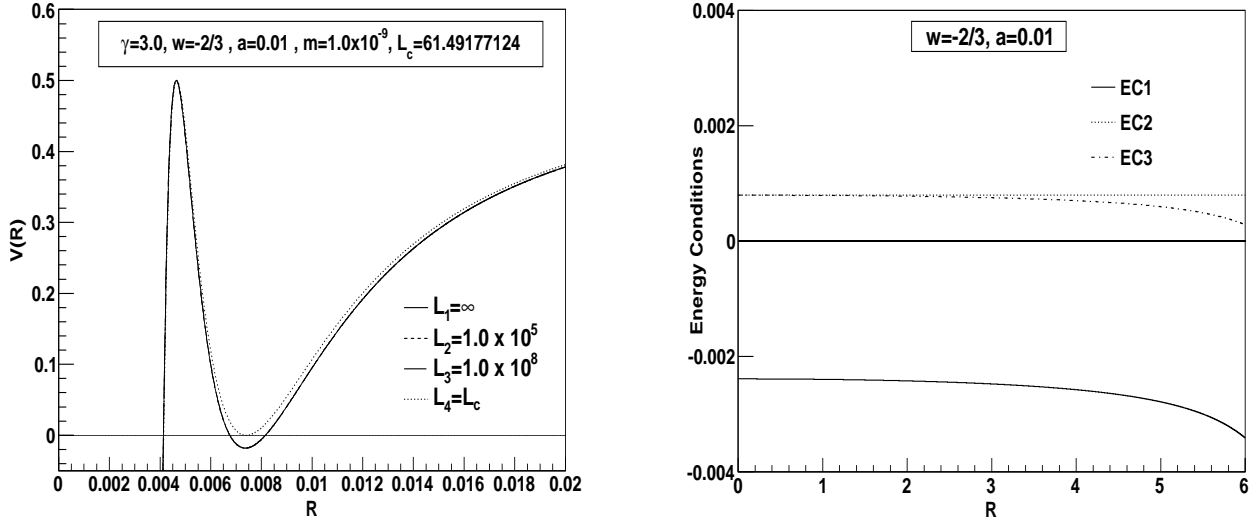


FIG. 4: The zoom of the potential $V(R)$ (figure 1) and the energy conditions $EC1 \equiv \rho + p_r + 2p_t$, $EC2 \equiv \rho + p_r$ and $EC3 \equiv \rho + p_t$, for $\gamma = 3$, $\omega = -2/3$, $a = 0.01$ and $m_c = 0.1054688609 \times 10^{-8}$. The horizons are: $r_h = 7.071067814$; $r_{bh} = -0.2368329842 \times 10^{-4}$, $r_c = 1.0 \times 10^5$ ($L_e = 1.0 \times 10^5$); $r_{bh} = -0.2368329842 \times 10^{-1}$, $r_c = 1.0 \times 10^8$ ($L_e = 1.0 \times 10^8$); $r_{bh} = -0.1456327969 \times 10^{-7}$, $r_c = 61.49177126$ ($L_e = 61.49177124$). Note that we have a gravastar enclosing a naked singularity. Then, for small R , the shell can collapse to form a naked singularity. **Case F**

- formation*,” J. Cosmol. Astropart. Phys. **12**, 17 (2009) [arXiv:gr-qc/09102054].
- [12] R. Chan and M.F.A. da Silva, ”How the charge can affect the formation of gravastars,” J. Cosmol. Astropart. Phys. **7**, 29 (2010) [arXiv:gr-qc/10053703].
- [13] R. Chan, M.F.A. da Silva and P. Rocha, ”Gravastars and Black Holes of Anisotropic Dark Energy” [arXiv:gr-qc/10094403].
- [14] R. Chan, M.F.A. da Silva, J.F. Villas da Rocha, ”Star Models with Dark Energy”, Gen. Relat. Grav. **41**, 1835 (2008) [arXiv:gr-qc/08033064]
- [15] O. Bertolami, J. Páramos, Phys. Rev. D **72**, 123512 (2005) [arXiv:astro-ph/0509547]
- [16] F. Lobo (2007) [arXiv:gr-qc/0611083].
- [17] C. Cattoen, T. Faber and M. Visser, Class. Quantum Grav. **22** 4189 (2005).
- [18] V. Dzhunushaliev, V. Folomeev, R. Myrzakulov and D. Singleton, Journal of High Energy Physics **7**, 94 (2008), [arXiv:gr-qc:08053211].

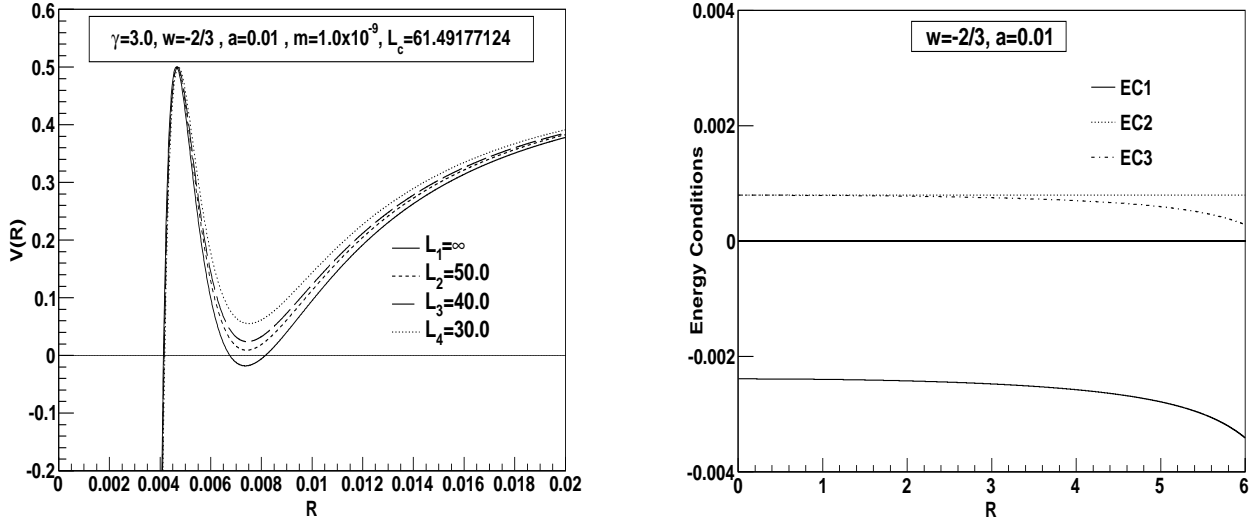


FIG. 5: The zoom of the potential $V(R)$ (figure 1) and the energy conditions $EC1 \equiv \rho + p_r + 2p_t$, $EC2 \equiv \rho + p_r$ and $EC3 \equiv \rho + p_t$, for $\gamma = 3$, $\omega = -2/3$, $a = 0.01$ and $m_c = 0.1054688609 \times 10^{-8}$. The horizons are: $r_h = 7.071067814$; $r_{bh} = -0.1184164921 \times 10^{-7}$, $r_c = 50.0$ ($L_e = 50$); $r_{bh} = -0.9473319370 \times 10^{-7}$, $r_c = 40$ ($L_e = 40$); $r_{bh} = -0.7104989528 \times 10^{-8}$, $r_c = 30.0$ ($L_e = 30$). Note that we have a gravastar enclosing a naked singularity. Then, for small R , the shell can collapse to form a naked singularity. **Case F**

- [19] F. Lobo, *Class. Quant. Grav.* **23**, 1525 (2006).
- [20] K. Lake, *Phys. Rev. D* **19**, 2847 (1979).
- [21] S.W. Hawking and G.F.R. Ellis, *The large scale structure of space-time* (Cambridge University Press, Cambridge, 1973).
- [22] R. Chan, M.F.A. da Silva, J.F. Villas da Rocha, *Mod. Phys. Lett. A* **24**, 1137 (2008) [arXiv:gr-qc/08032508].
- [23] S. Shankaranarayanan, *Phys. Rev. D.* **67**, 084026 (2003).

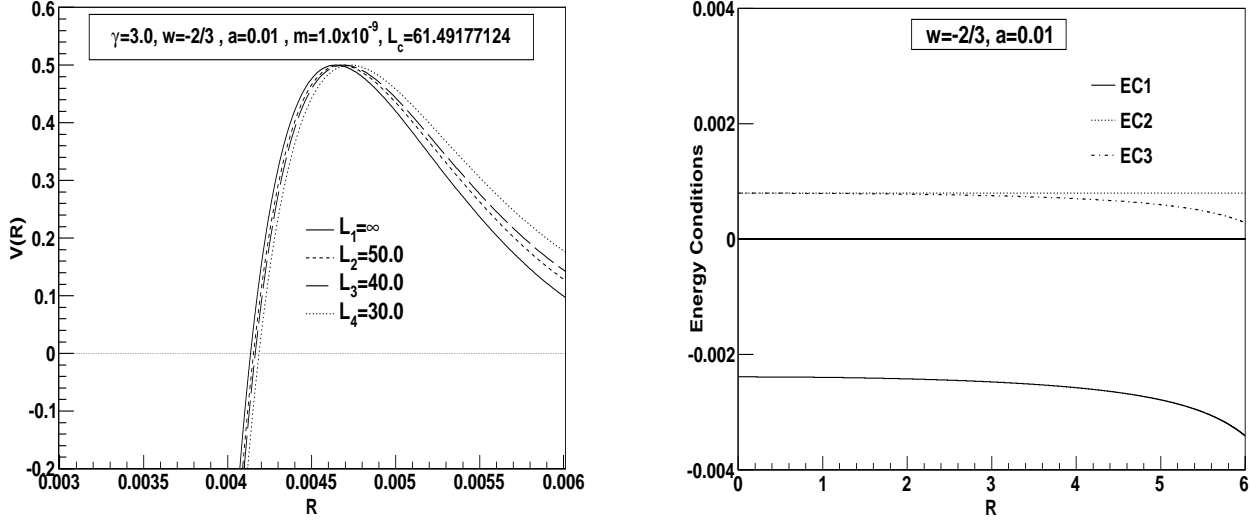


FIG. 6: The zoom of the potential $V(R)$ (figure 1) and the energy conditions $EC1 \equiv \rho + p_r + 2p_t$, $EC2 \equiv \rho + p_r$ and $EC3 \equiv \rho + p_t$, for $\gamma = 3$, $\omega = -2/3$, $a = 0.01$ and $m_c = 0.1054688609 \times 10^{-8}$. The horizons are: $r_h = 7.071067814$; $r_{bh} = -0.1184164921 \times 10^{-7}$, $r_c = 50.0$ ($L_e = 50$); $r_{bh} = -0.9473319370 \times 10^{-7}$, $r_c = 40$ ($L_e = 40$); $r_{bh} = -0.7104989528 \times 10^{-8}$, $r_c = 30.0$ ($L_e = 30$). Note that we have a gravastar enclosing a naked singularity. Then, for small R , the shell can collapse to form a naked singularity. **Case F**

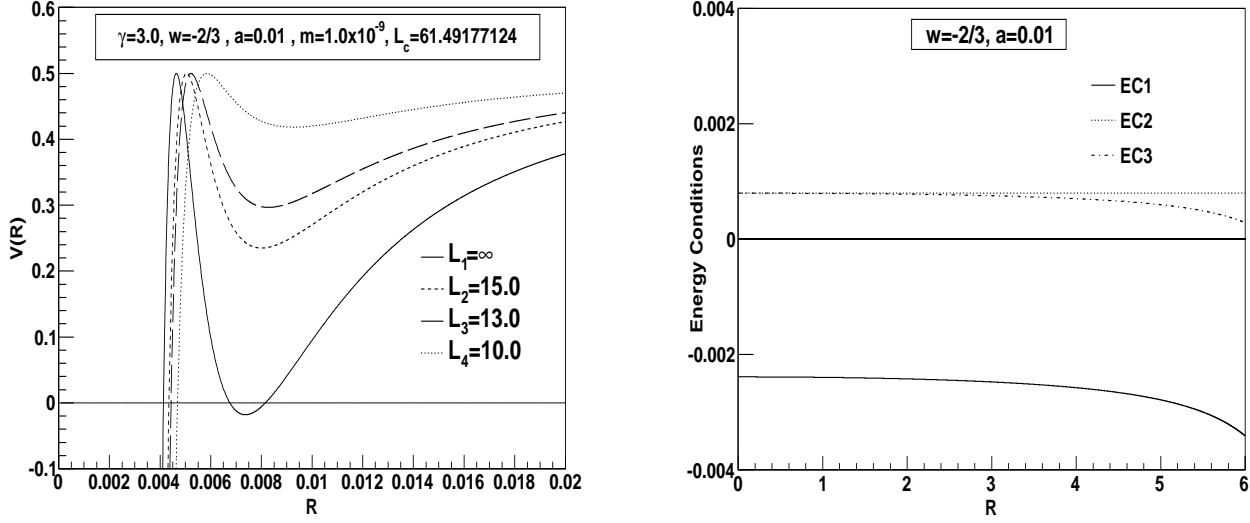


FIG. 7: The zoom of the potential $V(R)$ (figure 1) and the energy conditions $EC1 \equiv \rho + p_r + 2p_t$, $EC2 \equiv \rho + p_r$ and $EC3 \equiv \rho + p_t$, for $\gamma = 3$, $\omega = -2/3$, $a = 0.01$ and $m_c = 0.1054688609 \times 10^{-8}$. The horizons are: $r_h = 7.071067814$; $r_{bh} = 0.9178675538 \times 10^{-8}$, $r_c = 10.0$ ($L_e = 10$). Note that we have a gravastar enclosing a black hole. Then, for small R , the shell can collapse to form a black hole. **Case F**

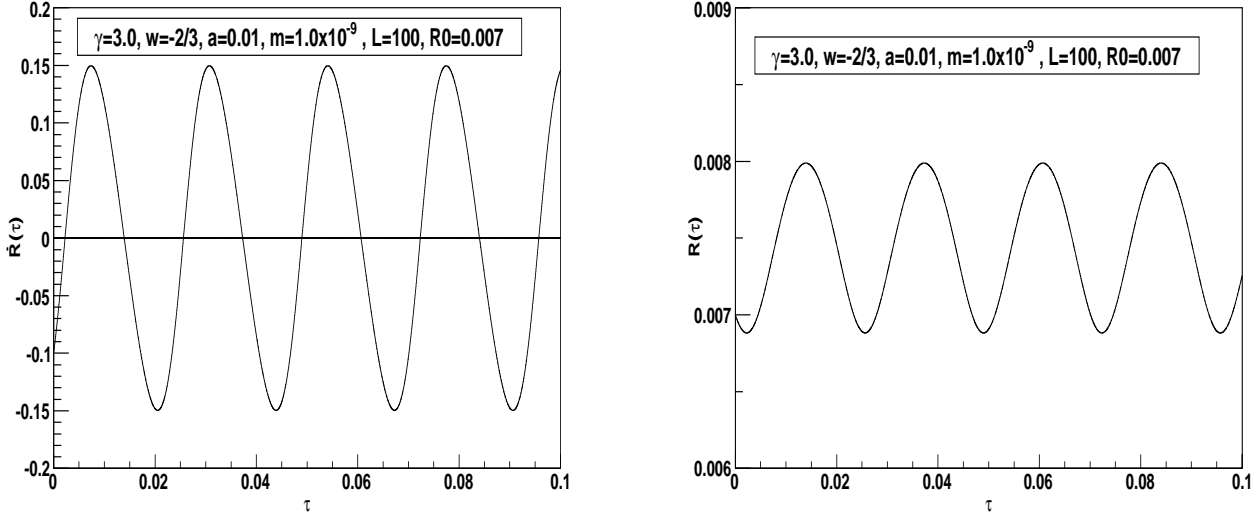


FIG. 8: These figures represent the dynamical evolution of a "bounded excursion" gravastar with the potential given by the figure 1, assuming $R_0 = R(0) = 0.007$.

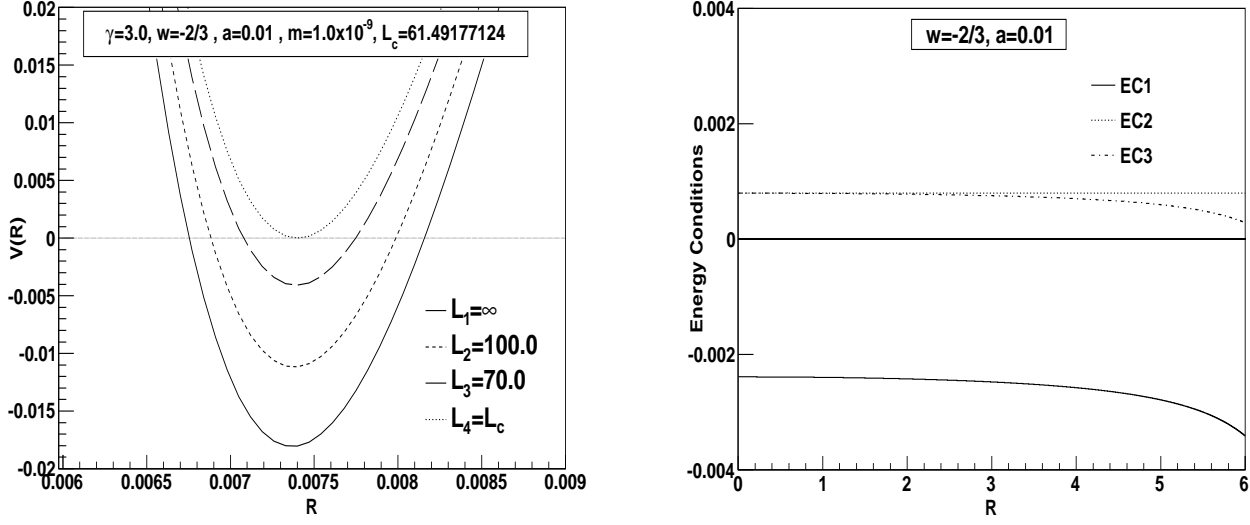


FIG. 9: Zoom of the potential $V(R)$ of figure 1 and the energy conditions $EC1 \equiv \rho + p_r + 2p_t$, $EC2 \equiv \rho + p_r$ and $EC3 \equiv \rho + p_t$, for $\gamma = 3$, $\omega = -2/3$, $a = 0.01$ and $m_c = 0.1054688609 \times 10^{-8}$. The horizons are: $r_h = 7.071067814$; $r_{bh} = -0.2368329842 \times 10^{-7}$, $r_c = 99.99999998$ ($L_e = 100$); $r_{bh} = -0.1657830889 \times 10^{-7}$, $r_c = 70$ ($L_e = 70$); $r_{bh} = -0.1456327969 \times 10^{-7}$, $r_c = 61.49177126$ ($L_e = 61.49177124$). **Case F**

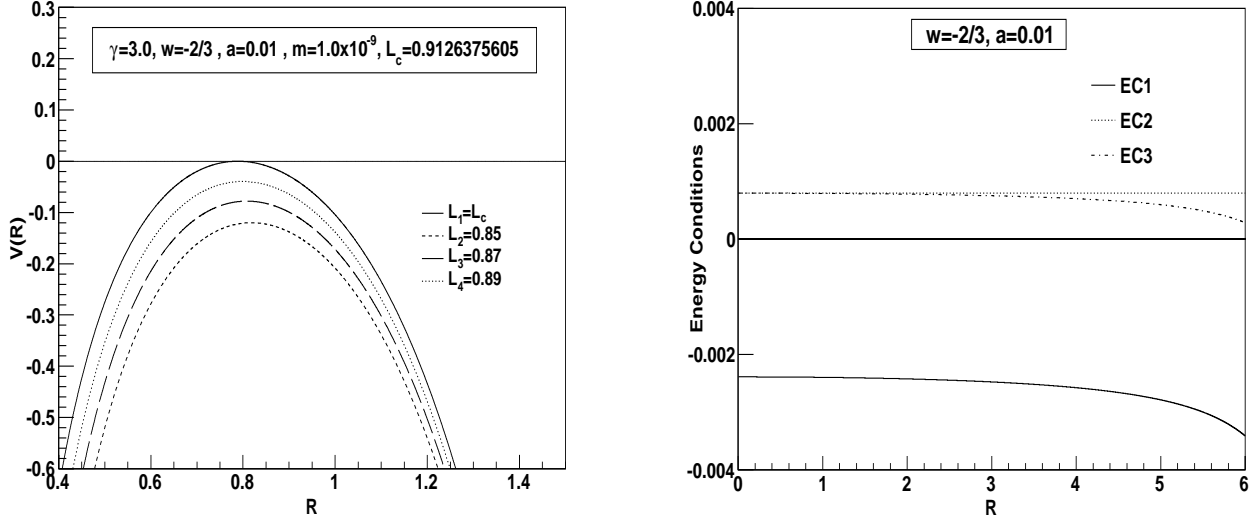


FIG. 10: The potential $V(R)$ and the energy conditions $EC1 \equiv \rho + p_r + 2p_t$, $EC2 \equiv \rho + p_r$ and $EC3 \equiv \rho + p_t$, for $\gamma = 3$, $\omega = -2/3$, $a = 0.01$ and $m_c = 0.1054688609 \times 10^{-8}$. The horizons are: $r_h = 7.071067814$; $r_{bh} = 0.1891503488 \times 10^{-8}$, $r_c = 0.9126375596$ ($L_e = 0.9126375605$); $r_{bh} = 0.1761682879 \times 10^{-8}$, $r_c = 0.8499999992$ ($L_e = 0.85$). **Case F**

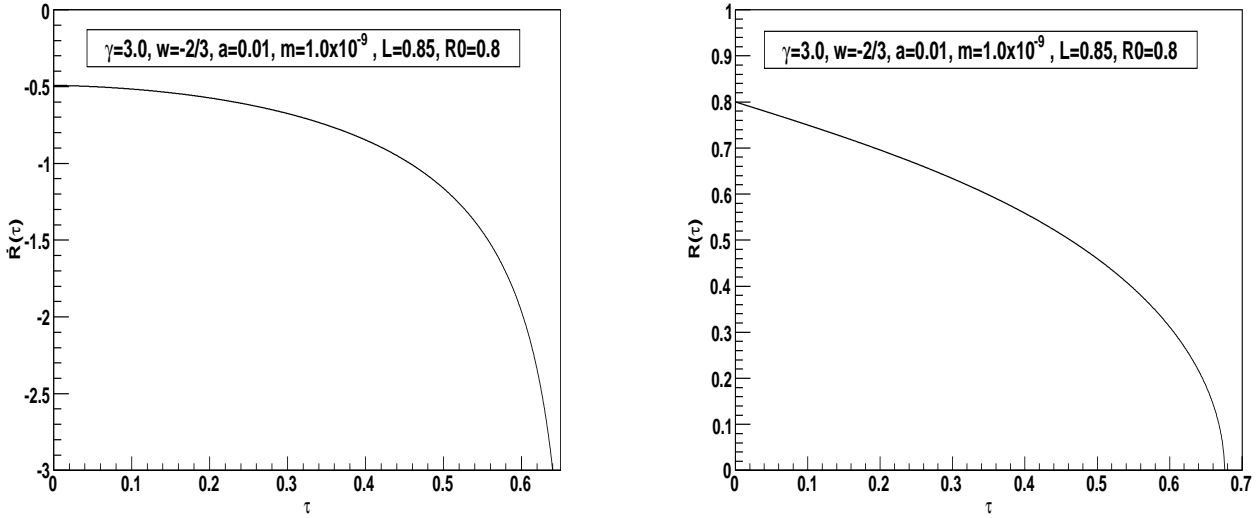


FIG. 11: These figures show the dynamical evolution of the collapse of a gravastar with the potential given by the figure 10, assuming $R_0 = R(0) = 0.9$, forming at the end of the evolution a black hole.

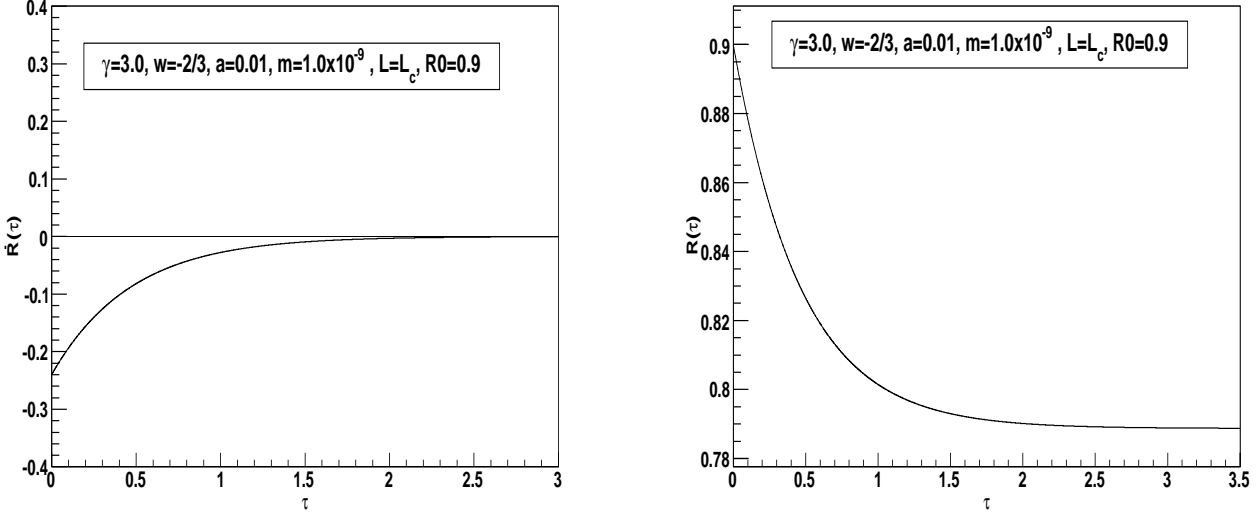


FIG. 12: These figures show the dynamical evolution of an unstable gravastar with the potential given by the figure 10, assuming $R_0 = R(0) = 0.9$.

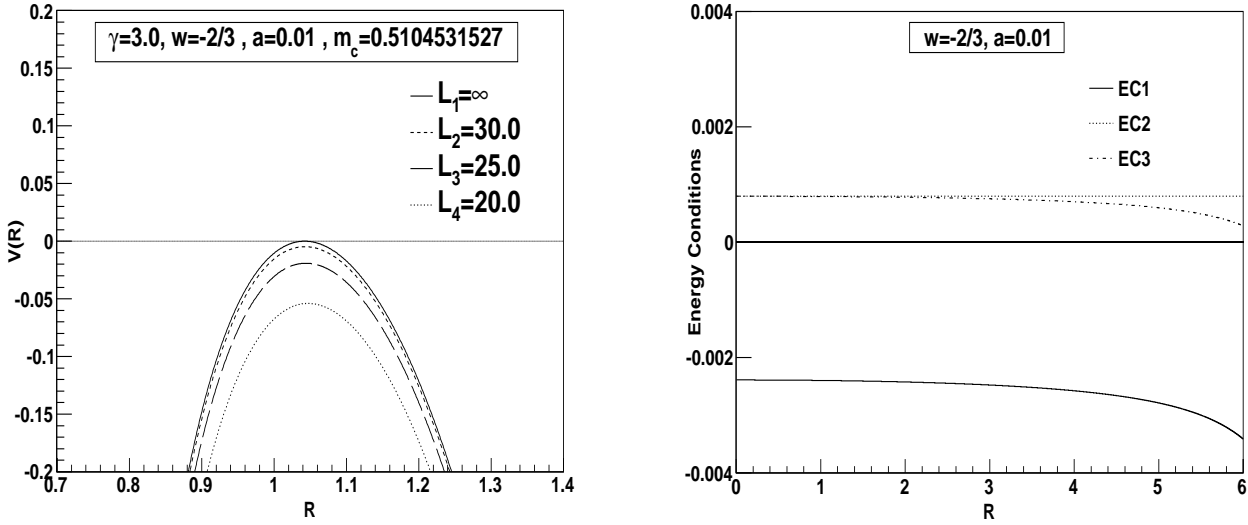


FIG. 13: The potential $V(R)$ and the energy conditions $EC1 \equiv \rho + p_r + 2p_t$, $EC2 \equiv \rho + p_r$ and $EC3 \equiv \rho + p_t$, for $\gamma = 3$, $\omega = -2/3$, $a = 0.01$ and $m_c = 0.5104531527$. The horizons are: $r_h = 7.071067814$; $r_{bh} = 1.022092711$, $r_c = 29.47589240$ ($L_e = 30$); $r_{bh} = 1.022617334$, $r_c = 24.47300022$ ($L_e = 25$); $r_{bh} = 1.023587410$, $r_c = 19.46855167$ ($L_e = 20$). **Case F**

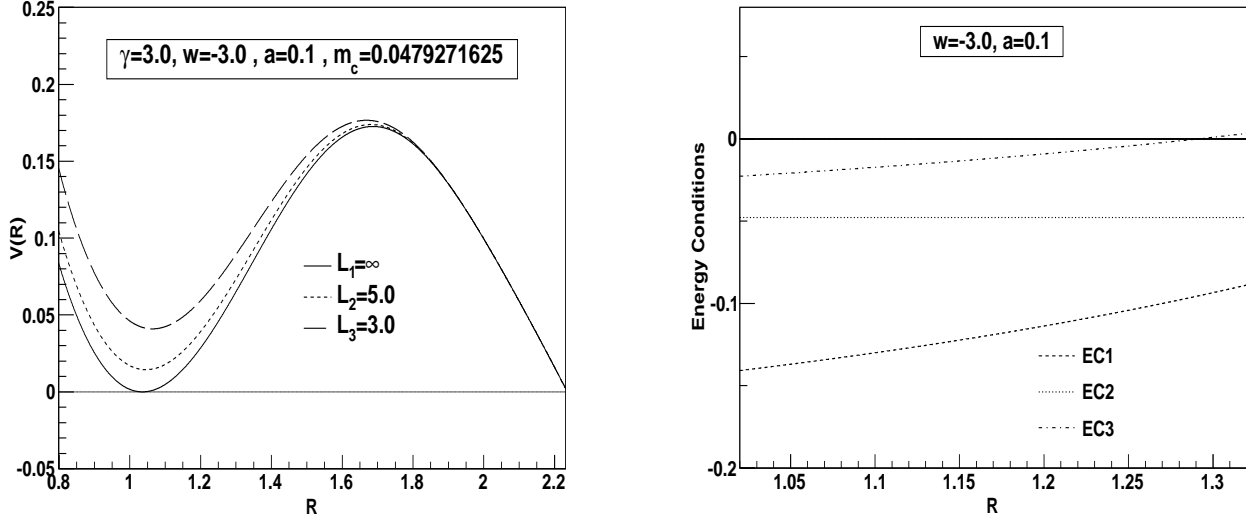


FIG. 14: The potential $V(R)$ and the energy conditions $EC1 \equiv \rho + p_r + 2p_t$, $EC2 \equiv \rho + p_r$ and $EC3 \equiv \rho + p_t$, for $\gamma = 3$, $\omega = -3$, $a = 0.1$ and $m_c = 0.0479271625$. The horizons are: $r_h = 2.236067977$; $r_{bh} = 0.09588959554$, $r_c = 4.951365546$ ($L_e = 5$); $r_{bh} = 0.09595248530$, $r_c = 2.950872678$ ($L_e = 3$).

Case I

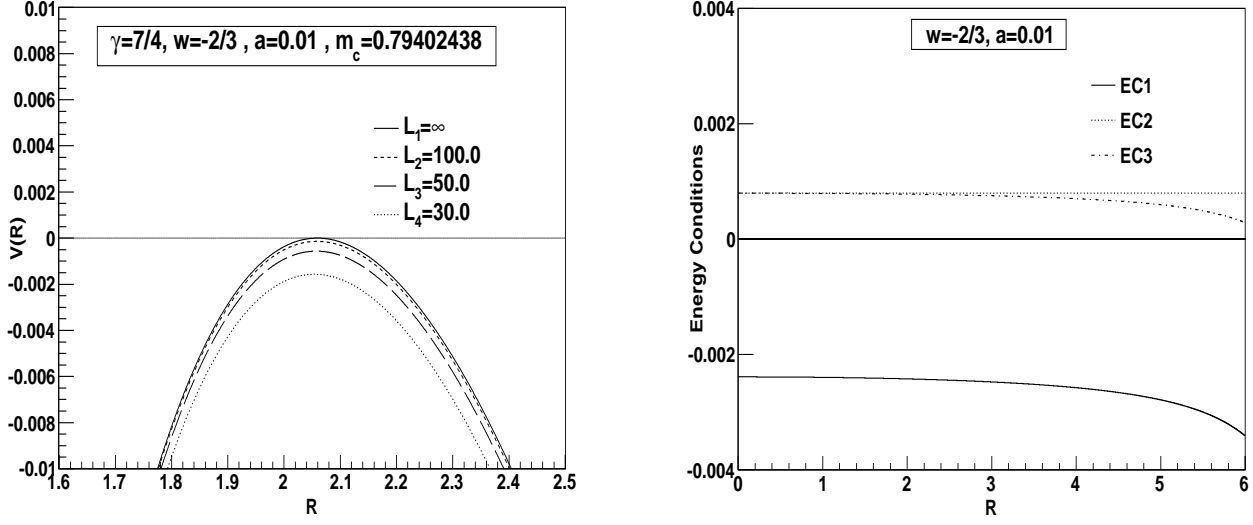


FIG. 15: The potential $V(R)$ and the energy conditions $EC1 \equiv \rho + p_r + 2p_t$, $EC2 \equiv \rho + p_r$ and $EC3 \equiv \rho + p_t$, for $\gamma = 7/4$, $\omega = -2/3$, $b = 0.01$ and $m_c = 0.79402438$. The horizons are: $r_h = 7.071067814$; $r_{bh} = 1.588449580$, $r_c = 99.19631286$ ($L_e = 100$); $r_{bh} = 1.589655604$, $r_c = 49.18621608$ ($L_e = 50$); $r_{bh} = 1.592536495$, $r_c = 29.17201284$ ($L_e = 30$). **Case E**

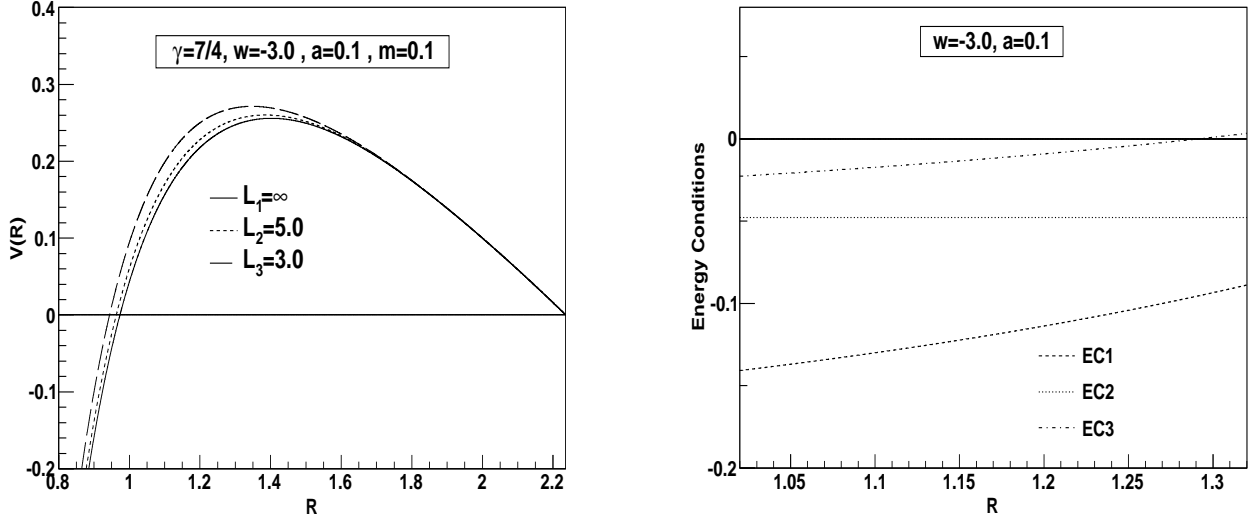


FIG. 16: The potential $V(R)$ and the energy conditions $EC1 \equiv \rho + p_r + 2p_t$, $EC2 \equiv \rho + p_r$ and $EC3 \equiv \rho + p_t$, for $\gamma = 7/4$, $\omega = -3$, $a = 0.1$ and $m_c = 0.1$. The horizons are: $r_h = 7.071067814$; $r_{bh} = 0.2003215448$, $r_c = 4.896828668$ ($L_e = 5$); $r_{bh} = 0.2009009580$, $r_c = 2.894500124$ ($L_e = 3$).

Case H